[11] Chang-Lin J.E., Attar M., Acheampong A.A., Pharmacokinetics and pharmacodynamics of a sustained-release dexamethasone intravitreal implant. Invest Ophthalmol Vis Sci. 52 (2011) 80-86.
[12] Jing Xu, Jeffrey J.H., Barocas V.H., Theodore W. R., Permeability and diffusion in vitreous humor: implications for drug delivery, Pharmaceutical Research, 17 (2000) 664-669.
[13] Kathawate J., Acharya S., Computational modeling of intravitreal drug delivery in the vitreous chamber with different vitreous substitutes, International Journal of Heat and Mass Transfer 51 (2008) 5598–5609.
[14] Lao L.L., Venkatraman S.S., Peppas N.A., Modeling of drug release from biodegradable polymer blends, European Journal of Pharmaceutics and Biopharmaceutics 70 (2008) 796–803.
[15] Stay M.S., Xu J., Randolph T.W., Barocas V.H., Computer simulation of convective and diffusive transport of controlled-release drug in the vitreous humor, Pharmaceutical Research, 20 (2003) 96-102.
[16] Rothstein S., Federspiel W., Little S., A unified mathematical model for the prediction of controlled release from surface and bulk eroding polymer matrices, Biomaterials 30 (2009) 1657–1664.
[17] Drug Product Development for the Back of the Eye, editors Uday B. Kompella, Henry F. Edelhauser (2011).
[18] Quarteroni A., Alberto V., Numerical approximation of partial differential equations, Springer (1994).
[19] Yew C.Y., Thomas P.,Ahmed K., Results of intravitreal dexamethasone implant 0.7 mg (Ozurdex) in non-infectious posterior uveitis International Journal of Ophthalmology vol. 8 (2015) 835-838.

J.A. Ferreira
CMUC-Department of Mathematics, University of Coimbra, Apartado 3008, 3001-454 Coimbra, Portugal
E-mail address: ferreira@mat.uc.pt
URL: http://www.mat.uc.pt/~ferreira

Paula de Oliveira
CMUC-Department of Mathematics, University of Coimbra, Apartado 3008, 3001-454 Coimbra, Portugal
E-mail address: email:poliveir@mat.uc.pt

P. da Silva
IPC/ISEC - Department of Physics and Mathematics, ISEC, Coimbra, Portugal
E-mail address: pascals@isec.pt

R. Silva
Department of Ophthalmology. Centro Hospitalar e Universitário de Coimbra (CHUC). Portugal Faculty of Medicine, University of Coimbra. Institute for Biomedical Imaging and Life Sciences (FMUC-IBILI). Portugal Association for Innovation and Biomedical Research on Light and Image (AIBILI). Coimbra. Portugal
E-mail address: rufino.silva@oftalmologia.co.pt

Pré-Publicações do Departamento de Matemática
Universidade de Coimbra
Preprint Number 17–57

TOWARDS A PRECISION OPHTHALMOLOGY: TARGETTING THE RETINA

J.A. FERREIRA, PAULA DE OLIVEIRA, P. DA SILVA AND R. SILVA

Abstract: Efficacious drug delivery to the posterior chamber of the eye is a very challenging problem due to the many physiological barriers that protect the eye against the entry of exogenous substances. To avoid, or to limit, the action of these barriers several drug delivery routes are being investigated and used in clinical opthalmology. To assist medical and pharmaceutical research, mathematical modelling of the release kinetics assumes a crucial role. In this paper three dimensional computational models that simulate drug delivery from two different biodegradable polymeric platforms - intravitreal and transscleral - are presented. The models consist of coupled systems of partial differential equations linked by interface conditions, where the properties of the drug, of the implant and of the eye tissues are taken into account. Peak concentrations and residence times are compared for the two delivery routes. Particular attention is devoted to the modelling of the Blood Retinal Barrier (BRB). The influence of retinal diseases, represented by parameters that characterize the permeation through the BRB, is analyzed. Numerical simulations that illustrate the differences in the behavior of drug released from intravitreal and transscleral implants are included.

Key words: Partial Differential Equations, Drug Delivery, Retina

Mathematics Subject Classification (2000): 65M06, 65M20, 65M15

1. Introduction

One of the major challenges faced nowadays by pharmacology is drug delivery to the posterior chamber of the eye. The reason for this fact is the existence of different static and dynamic barriers that hinder the release of drugs to the retina ([2]). The cornea, the conjuntiva, the sclera and the retinal pigmental epitehelium (RPE) are physical barriers while drug clearance mechanisms through blood and lymphatic vessels are dynamic barriers (Figure 1).

Several routes of administration can be used to target the retina as the topical, the systemic, the intravitreal or the transscleral among others. When assessing the efficacy of these routes the effectivness of the main barriers the drug encounters, must be evaluated.

Received December 28, 2017.

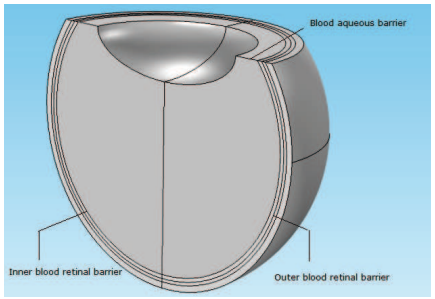

FIGURE 1. Blood Barriers in the human eye.

It is estimated that only 5% of a dose administrated by the topical route penetrates into the eye, and that only a negligible amount reaches the posterior segment. The permeation of drug is hindered by different barriers of the anterior eye, as the low permeability of the cornea, the loss through the nasolacrimal duct and the blood aqueous barrier. Furthermore the distance the drug should diffuse to reach the retina explains that the topical route is not effective in retinal pathologies. The systemic administration is limited by the degradation of drugs before reaching the target, but also by the inner blood retinal barrier (inner BRB) and the outer blood retinal barrier (outer BRB). The Blood Retinal Barriers (BRB's) limit the passage of molecules and ions through the space between cells: the inner BRB is formed of tight junctions between the cells that cover the retinal capillaries; in the outer BRB tight junctions are located between retinal pigment epithelial cells ([2]). To overcome these barriers higher doses should be administrated which is not admissible due to the possible occurrence of adverse side effects.

The difficulties of the classical routes -topical and systemic- have boost the development of alternative drug delivery systems whose target is the retina. The idea underlying these systems is to deliver the drug as close the target tissue as possible. One possibility is to install a delivery device intended for sustained release from biodegradable or non-biodegradable polymeric matrices over long periods of time. The aim of this paper is to model mathematically drug delivery from two such devices: intravitreal and transscleral implants (Figure 2). Two particular aspects are addressed: the quantitative and qualitative behaviour of drug concentration in the vitreous and the

by a factor of ten the peak concentration decreases 22%; when $A_{r,c}$, the parameter that represents the integrity of the outer BRB, is multiplied by a factor of 10 the peak concentration is approximately multiplied by 7 (Figure 13 and Figure 14). The previous arguments suggest that while transscleral delivery is sensitive to inner BRB breakdown and very sensitive to the outer BRB breakdown, the concentration levels in the case of intravitreal release do not respond to BRB's leakage.

Acknowledgements

This work was partially supported by the Center for Mathematics of the University of Coimbra - UID/MAT/00324/2013, funded by Portuguese Government through FCT/MEC and co-funded by through the Partnership Agreement PT 2020.

The authors are grateful to Rui Bernardes for helpful discussions.

References

[1] Cunha-Vaz J., Bernardes R., Lobo C., Blood-retinal barrier, European Journal of Ophthalmology, 21 (2011) 3-9.
[2] Ryan S.J., Schachat A.P., Wilkinson C.P. , Hinton D.R., Sadda S.R., Retina, 5th Edition, 2012.
[3] Mac Gabhann F., Demetriades A.M., Deering T., Packer J.D., Shah S.M., Duh E., Campochiaro P.A., Popel A.S., Protein transport to choroid and retina following periocular injection: theoretical and experimental study, Annals of Biomedical Engineering, 2007, 35(4), 615-30.
[4] Balachandran R.K., Barocas V.H., Computer modeling of drug delivery to the posterior eye: effect of active transport and loss to choroidal blood flow, Pharmaceutical research, 25 (2008) 2685-2696.
[5] Causin P., Malgaroli F., Mathematical assessment of drug build-up in the posterior eye following transscleral delivery, Journal of Mathematics in Industry, (2016) 6-9.
[6] Shah J.N., Shah H.J., Groshev A., Hirani A.A., Pathak Y.V., Sutariya V.B., Nanoparticulate transscleral ocular drug delivery, Journal Biomolecular Research & Therapeutics, Volume 3, Issue 3, (2014).
[7] Andrew R.H. Simpson, Robert Petrarca, Timothy L. Jackson, Vitreomacular adhesion and neovascular age-related macular degeneration, Survery of Ophthalmology, 57 (2012) 498-509.
[8] Chan A., Loh-Shan L., Mark S.B., Critical appraisal of the clinical utility of the dexamethasone intravitreal implant (Ozurdex) for the treatment of macular edema related to branch retinal vein occlusion or central retinal vein occlusion, Clin Ophthalmol, 5 (2011) 1043-1049.
[9] Ferreira J.A., Paula de Oliveira, Silva P.M., Silva R., Mathematics of aging: Diseases of the posterior segment of the eye, Computers and Mathematics with Applications, 73, (2017) 11-26.
[10] Azhdari E., Ferreira J.A., Oliveira P., Silva P.M., Diffusion, viscoelasticity and erosion: analytical study and medical applications, Journal of Computational and Applied Mathematics, 275 (2015) 489-501.

by addressing a pure mathematical question regarding the well-posedeness of the model system of equations (1)-(8), which we answer in Section 3. We established that the model is stable, under perturbations of the initial data, for finite intervals of time and that it has a unique weak solution.

From a computational viewpoint the aim of the study presented here was to carry on simulations that could answer to the following questions:

1. How can we compare the distribution of drug eluted from intravitreal and transscleral implants, regarding peaks and residence time?
2. How does the inner and outer BRB's breakdown affect drug distribution in the case of intravitreal delivery?
3. How does the inner and outer BRB's breakdown affect drug distribution in the case of transscleral delivery?

The values of the parameters used in the simulations have been gathered from the literature ([3], [4], [13]). Regarding 1 drug distribution in the retina was simulated for both delivery systems and considering the same initial amount of drug in both systems. For the intravitreal route a peak of $1.48 \times 10^{-3}\ mol/mm^3$ was observed after 12 days while in the case of the transscleral route the peak of concentration is observed after 3.8 hours and the highest value of drug concentration achieved is $1.4 \times 10^{-4}\ mol/mm^3$ ($\gamma_{r,1} = 10^{-4}$, $A_{r,c} = 10^{-8}$). These results suggest that a large amount of drug is lost from the scleral surface and through the choroidal circulation.

Concerning question 2 we concluded that the release of drug from the intravitreal implant is not very sensitive to the breakdown of the inner BRB. We observed (Figure 11) that when γ_r, the parameter that controls the breakdown of the inner BRB, is decreased by a factor of 10 times then the peak concentration, attained after 12 days, increases 28%. This means that in pathologies characterized by the breakdown of the inner BRB, as diabetic retinopathy ([1]), more severe is the patient condition less efficacious is the delivery. The sensivity of the intravitreal route relatively to the leakage of cells that form the outer BRB is not very significant as can be observed in Figure 12. When the parameter $A_{r,c}$, which controls the breakdown of the outer BRB, is increased by a factor of 10 the concentration peak remains approximately constant. As a consequence the efficacity of drug delivery in patients with age-related macular degeneration , characterized by a breakdown of the outer BRB, does not appear affected.

The answer to question 3 reveals that the breakdown of BRB's induces different behaviors in the case of a transscleral implant. When γ_r is increased

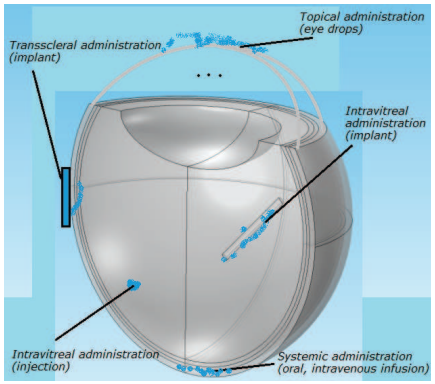

FIGURE 2. Routes of drug administration.

retina, and the influence of blood barriers leakage, that occurs in most retinal pathologies.

An *a priori* analysis of the barriers that the drug must face, before targetting the retina, suggests that the intravitreal route should lead to higher concentrations ([6]). In fact it elliminates all physical and all dynamical barriers while, drug administered by the transscleral route, must cross the sclera, face the clearance of the choroid, permeate the Retinal Pigment Epithelium (RPE) and overcome active pumping - a mechanism responsible for moving toxic substances out of the retina (Figure 3). Overall, when compared with other routes, the intravitreal route is generally considered by clinicians as the best, in terms of efficacy but the worst in terms of safety with the possible occurrence of potential severe complications such as endophthamitis or retinal detachment among others. When the transscleral route is used steep concentration gradients occur: the highest concentration develops at the sclera and the lowest concentrations in the vitreous and the retina.

The use of biodegradable implants is successfully used to treat serious intraocular disorders. The intravitreal implant is expected to release higher concentrations of drug in the retina, but the procedure is very invasive possibly causing adverse events; the transscleral implant is safer but it is expected that they reach lower concentration levels. In fact the drug eluted from a transscleral implant doesn't bypass the blood-retinal barrier with minimal systemic absorption, as in the case of the intravitreal implant. However

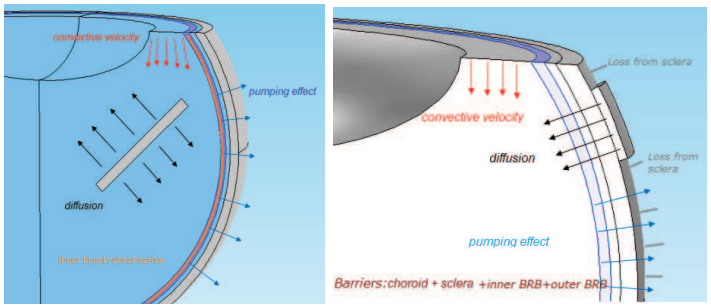

FIGURE 3. Scheme of the barriers drug delivery must face: drug released from an intravitreal implant reaches the retina without passing through the BRB's (left); drug released through the transscleral route crosses the sclera, the choroid and the RPE against the action of efflux pumps.

only by a computational approach it is possible to compare the behavior of drug concentration released by both systems. In fact direct measurements of concentrations levels are made only in experiments with animal models. Ophthalmologists analyze the efficacy of the route by measuring the visual acuity through the increase in the number of letters from baseline, during the follow up visits. We believe that a quantitative assessment, namely the computation of the peak and the residence time, can be useful in assisting clinicians when deciding between the intravitreal and the transcleral route.

The release of drug from the two routes - intravitreal and transscleral- depends not only on the barriers met by each route but also on the health conditions of the retina. One of the aspects that has a major influence on the release behaviour is the blood retinal barrier (Figure 1). The integrity of BRB plays a crucial role in the health of retina. The most frequent retinal diseases - diabetic retinopathy and age-related macular degeneration - are associated to BRBs breakdown. Understanding the influence of BRB's alterations on drug distribution is essential to develop strategies to deliver drug to the retina. Several authors have proposed mathematical models of drug delivery to the posterior segment of the eye. Regarding the intravitreal route we mention [13] where drug distribution from an intravitreal injection is studied. Concerning transscleral release we mention without being exhaustive [4] and [5]. In [4] the authors present a 3D model of drug distribution in the vitreous, retina and a choroid-sclera unique layer. They compare systemic with transscleral release: in the first case the release is represented by a source term in the coroid-sclera

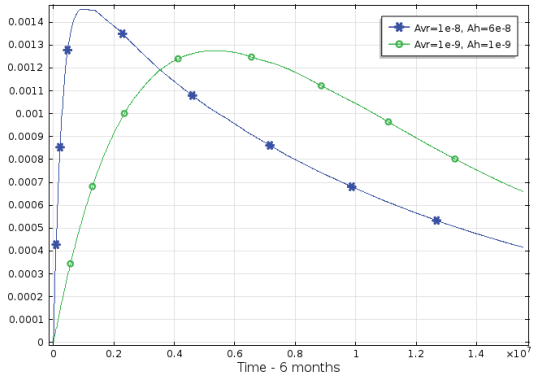

FIGURE 16. Drug concentration in the retina during 6 months: influence of the hyaloid permeability and of the permeability of the interface vitreous/retina.

In Table III we present a synthesis of some of the numerical results obtained.

Table III: Intravitreal route: Influence of parameters $A_{v,r}$ and A_h on the concentration peak and it's occurrence in the retina.

$A_{vr} \setminus A_h$	6×10^{-8}	10^{-9}
10^{-8}	$1.48 \times 10^{-3}\ mol/mm^3$ - 12 days	$1.95 \times 10^{-3}\ mol/mm^3$ - 17 days
10^{-9}	$4.2 \times 10^{-4}\ mol/mm^3$ - 32 days	$1.27 \times 10^{-3}\ mol/mm^3$ - 62 days
10^{-10}	$5.5 \times 10^{-5}\ mol/mm^3$ - 36 days	$3.6 \times 10^{-4}\ mol/mm^3$ - 155 days

5. Final Remarks

Ocular drug delivery is a major challenge to pharmacologists, clinicians and drug delivery scientists due to the hindrances caused by several ocular barriers. Drug delivery to the retina is an active area of research and is presently under intense investigation. As testing of tissue drug levels in humans is usually not possible, computer modelling techniques are an important tool as they can provide information and guidance for further clinical and laboratorial experiments and can assist in the rational design of new drug delivery systems.

We presented a mathematical model, represented by five coupled systems of PDE's that describe the distribution of drug eluted from biodegradable intravitreal and transscleral implants. After presenting the model we begin

retina and vitreous humor for 6 months, with peak concentrations at about 2 months ([19]). Regarding humans the peak is also referred to be attained by the second month. In this case the peak is measured by the best visual acuity achieved through the increase in the number of letters from baseline ([19]). In the numerical results presented in Section 4.1 and 4.2 the peak is achieved earlier, by the middle of the first month. We carried on a large number of experiments to delay the occurrence of the peak by considering small perturbations in the parameter values, that were gathered from the literature.

If only the permeability of the hyaloid membrane is decreased the peak increases but no delay is observed (Figure 15 -left). On the contrary if only A_{rv} is decreased then the occurrence of the peak is delayed (Figure 15 - right).

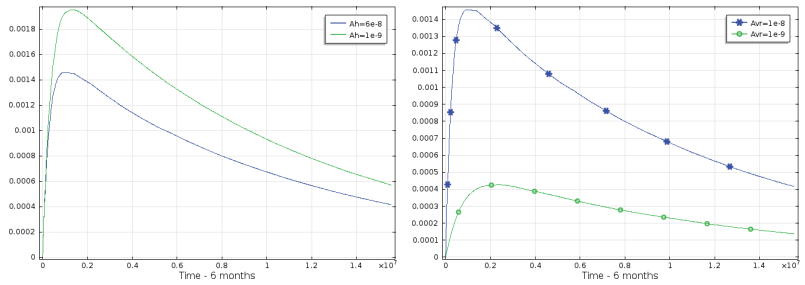

FIGURE 15. Drug concentration in the retina during 6 months: influence of the hyaloid permeability (left - $A_{vr} = 10^{-8}$) and of the permeability of the interface vitreous/retina (right - $A_h = 6 \times 10^{-8}$).

We exhibit in Figure 16 the simultaneous influence of both parameters. The concentration peak in this case is observed after 2 months. The result is in agreement with values presented in the literature ([11]) for the commercialized device.

layer; in the transscleral route drug release is represented through a boundary condition defined by a constant concentration located on the surface of the sclera. The effect of the BRB and the active pumping by the retina are taken into account. The main finding of the paper is that loss to the choroidal circulation is small compared to loss from the scleral surface. In [5] a model to compute drug concentration released from a transscleral implant is presented. The model is one dimensional and the posterior chamber is represented by the union of four different layers: vitreous, retina, choroid and sclera. The influence of the inner and outer BRB is taken into account. The feed of drug is modelled by a boundary condition represented by a decreasing exponential function acting on the surface of the sclera. Theoretical estimates for the L^2 norm of the concentration in the retina are also presented. A very complete list of references, on drug delivery to the posterior chamber, is contained in [4] and [5].

In a previous paper by the authors ([9]) the release from an intravitreal biodegradable implant is modelled. A mathematical model of an aging eye with a liquefying vitreous is introduced and the influence of retinal diseases and aging changes are analyzed. A two-dimensional geometry, obtained by cutting the eye ball by a plan that contains its center and the axis of the cylindrical intravitreal implant is considered. In [9] the results obtained for the concentrations have essentially a qualitative character because the two-dimensional section used is not representative of all great circles of an eye ball where an intravitreal implant is inserted.

In the present paper a three-dimensional model of the eye is considered and a comparison between the transscleral and the intravitreal routes is presented. The domain is composed by a biodegradable polymeric implant, and the different tissues of the posterior segment of the eye: vitreous, retina, choroid and sclera. When compared to [9], the present paper represents an improvement as it presents a comparison between intravitreal delivery and transscleral delivery, and this last route was not considered in [9]. Moreover the fact that the model is tridimensional leads to more accurate values of the concentration in the different tissues. Besides the differences in the mathematical model of the intravitreal implant, when compared to [9], two other contributions of the present paper are the following:

(i) the comparison of drug delivery behavior between intravitreal and transscleral routes;
(ii) the influence of eye pathologies in the delivery behavior of both routes.

Regarding the first aspect we observe that the transscleral implant is modelled by a realistic polymeric biodegradable matrix containing the same amount of drug as the intravitreal implant. In [4] and [5] the transscleral release of drug is prescribed by a boundary condition on the external surface of the sclera: a constant source in the case of [4] and a concentration exponentially decreasing in time in [5]. Concerning the second aspect we note that most retinal pathologies are accompanied by a breakdown of the blood retinal barriers (Figure 1): in the diabetic retinopathy the breakdown begins in the inner BRB; in age-related macular degeneration the breakdown occurs firstly in the outer BRB. The analysis of the breakdown of the inner and outer BRB's leads to meaningful qualitative and quantitative results: the breakdown of the outer BRB affects essentially transscleral release, while the breakdown of the inner BRB hinders mainly the intravitreal drug delivery.

In Section 2 we present the tridimensional geometry of the model and the coupled systems of partial differential equations that describe the release of drug in the different tissues of the posterior chamber, through an intravitreal or a transcleral biodegradable polymeric implant. A stability study is presented in Section 3. In Section 4 we exhibit numerical simulations of drug concentration and study its dependence on the values of physiological parameters. The release of drug through the intravitreal and the transscleral routes are addressed. The peak concentration and the residence in the retina are compared for both routes. The influence of the breakdown of BRB's is analysed for both routes. In Section 5 we present some final remarks.

2. Mathematical model

2.1. 3D Geometry of the model. The vitreous chamber is represented in Figure 4 by Ω_v. In normal conditions it is filled with vitreous humor and it occupies about two-thirds of the eye. The lens, also called crystalline lens, acts to focus images in the retina. It is modeled by an ellipsoid. The anterior hyaloid membrane and the lens separate the anterior chamber and the posterior chamber of the eye from the vitreous chamber. The vitreous humour is a transparent gel that fills the eye between the lens and the retina. It is a highly hydrated tissue, with a water content of around 99%. The retina, Ω_r, is the light sensitive layer of tissue that borders the posterior part of the eye. It is modeled as the volume between two spherical surfaces with radius differing of 0.2 mm and where the radius of the spherical vitreous chamber is 11 mm. We assume that the retina is a porous tissue. A capillary

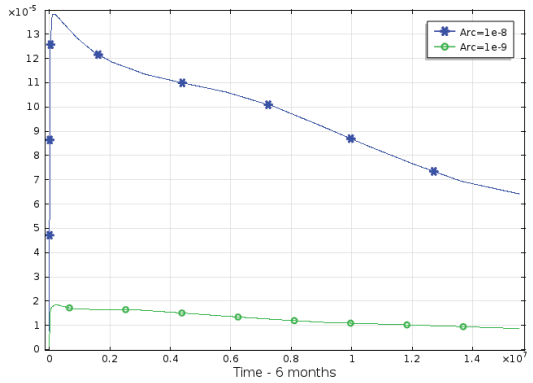

FIGURE 14. Influence of the breakdown of the outer BRB on the mean of drug concentration in the retina during 6 months, for two values of $A_{r,c}$, when a transscleral implant is used.

retina. In fact, a bigger $A_{r,c}$ implies less opposition to the permeation of drug. In the plot of Figure 14 a value of $A_{r,c}$ three times larger leads to a peak of concentration also three times higher. We note that in the case of intravitreal administration the accumulation of drug in the retina is not very sensitive to $A_{r,c}$ (Figure 12).

In Table II a synopsis of the results in Section 4.3 is presented.

Table II: Concentration peak in the retina (mol/mm^3) for the intravitreal and the transscleral routes.

	Inner BRB		Outer BRB	
	$\gamma_r = 10^{-5}$	$\gamma_r = 10^{-4}$	$A_{r,c} = 10^{-9}$	$A_{r,c} = 10^{-8}$
Intravitreal route	1.9×10^{-3}	1.48×10^{-3}	1.58×10^{-3}	1.48×10^{-3}
Transscleral route	1.78×10^{-4}	1.4×10^{-4}	1.8×10^{-5}	1.4×10^{-4}

4.4. A note on the peak concentration of the intravitreal implant. In the case of the intravitreal route the implant simulated in this paper has the characteristics of a commercial device approved in 2009 by the Food and Drugs Administration. This device is based on a PLGA poly(lactic-co-glycolic acid) polymeric implant where dexamethasone is dispersed. The parameters used in this paper to characterize the biodegradable polymer correspond to PLGA poly(lactic-co-glycolic acid). The parameters used for the drug correspond to dexamethasone. It is currently reported in the literature that in laboratorial experiments with animals, the drug is detected in the

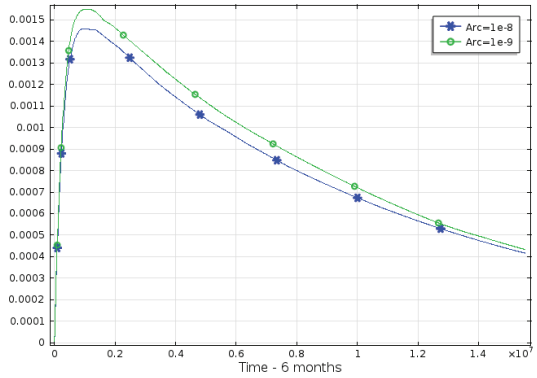

FIGURE 12. Influence of the breakdown of the outer BRB on the mean drug concentration in the retina during 6 months for two different values of $A_{r,c}$, when a intravitreal implant is used.

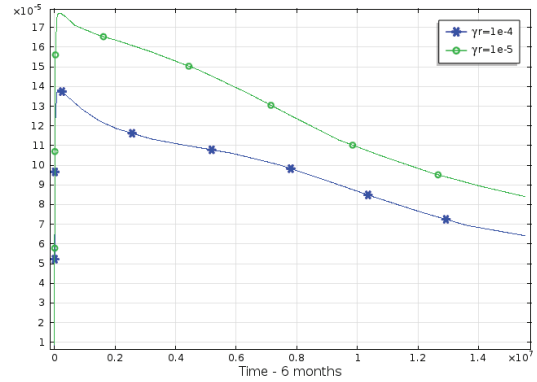

FIGURE 13. Influence of the breakdown of the inner BRB on the mean of drug cnoncentration in the retina during 6 months, for two different values of γ_r, when a transscleral implant is used.

increasing of drug concentration in the retina because less concentration is lost through the inner retinal vasculature.

The influence of the breakdown of the outer BRB, represented by the parameter $A_{r,c}$, is illustrated in Figure 14 for $A_{r,c} = 10^{-8}$, 10^{-9}. As the breakdown of the outer BRB progresses higher levels of drug are achieved in the

network is embedded in the inner retinal region. The inner BRB comprises the endothelium which lines these capillaries.

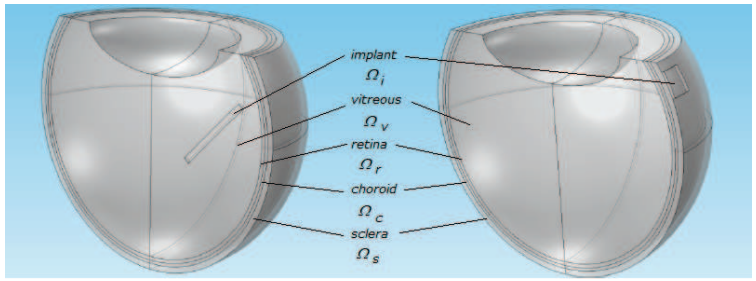

FIGURE 4. Geometry of the eye with an intravitreal implant (left) and with a transscleral implant (rigth): the polymeric device Ω_i, the vitreous humor Ω_v, the retina Ω_r,the choroid Ω_c and the sclera Ω_s.

The outer layer of the entire eyeball is the sclera, Ω_s, which contains collagen and elastic fibers and has a protective function. Between the retina and the sclera there is a vascular layer, the choroid, represented by Ω_c, containing blood vessels that nourish the retina. The interface between the retina and the choroid, which is called the Retinal Pigment Epithelium (RPE), is represented by $\Gamma_{r,c}$. The cells of the RPE - that form the outer Blood Retinal Barrier - are linked by tight junctions which act as a barrier against the diffusion of the solutes and nutrients from the choroid.

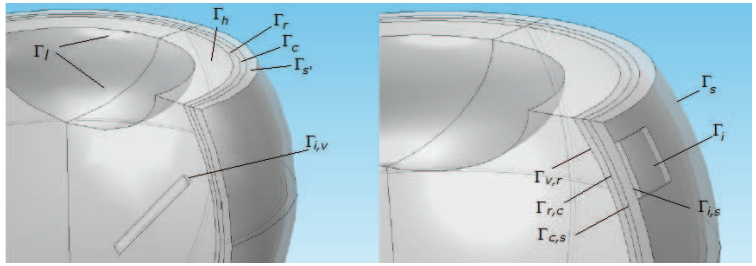

FIGURE 5. Interfaces and bounadaries

In Figure 4 (left) we represent an intravitreal biodegradable implant, Ω_i, containing dispersed drug, that is placed in the vitreous near the retina. It is geometrically represented by a polymeric cylinder with radius 0.023 mm and

height 0.6 mm. These dimensions correspond to a specific commercialized intravitreal drug delivery implant ([8], [19]).

In Figure 4 (right) the geometry for the release of drug through the transscleral route is illustrated. A patch like implant, Ω_i, is represented by a biodegradable polymeric paralelipiped with dimensions $3.2mm \times 2.6mm \times 0.2mm$. These dimensions do not correspond to any commercialized device. They have been considered as to guarantee that both implants-intravitreal and transscleral - are loaded with the same amount of drug.

2.2. Model equations. An initial amount of solid drug is dispersed in a biodegradable polymeric device: intravitreal or transscleral. We suppose that when the implant enters in contact with the vitreous or the sclera, depending on the type of administration, intravitreal or transscleral respectively, an instantaneous swelling of the platform occurs. The drug then dissolves and is transported by several mechanisms until it reaches the retina.

2.2.1. *Drug release from an intravitreal implant.* In the case drug is released from an intravitreal implant, Figure 4 (left), we summarize those mechanisms as follows:

(i) In the biodegradable implant (Ω_i): diffusion of the drug and biodegradation of the polymer;
(ii) In the vitreous humour (Ω_v): diffusion in the porous vitreous, convective transport due to a pressure gradient between the anterior part of the vitreous chamber and its posterior part, clearance through the hyaloid membrane;
(iii) In the retina (Ω_r): diffusion, convection, active pumping, clearance through the inner BRB, permeation through the outer BRB;
(iv) In the choroid (Ω_c): convective transport and clearance;
(v) In the sclera (Ω_s): diffusive transport.

We observe that the influence of convection on the kinetics of drug in the vitreous humor has been studied in [12] and [15]. The mathematical model that describes (i)-(v) results from the coupling of five systems of partial differential equations, representing the transport of drug in the five different regions Ω_i, Ω_v, Ω_r, Ω_c and Ω_s. These domains are considered homogeneous and isotropic. In a previous work by the authors ([9]) the vitreous (Ω_v) is considered heterogeneous to simulate liquefaction which is a common aging

To analyse the influence of the breakdown of the inner BRB on drug distribution we consider different degrees of severity of the pathology, represented by the value of the parameter γ_r (see (5)). The influence of the breakdown of the outer BRB is represented in our model, by the permeability parameter $A_{r,c}$ (see (14)), that regulates the drug flux between the retina and the choroid.

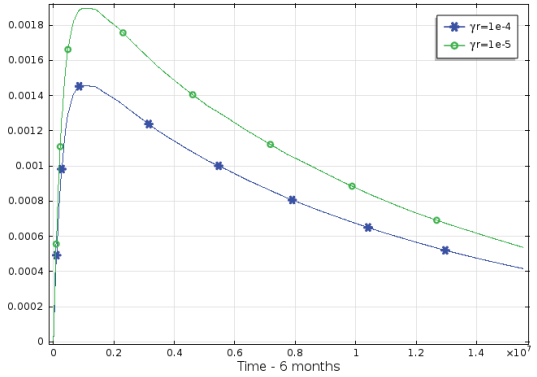

FIGURE 11. Influence of the breakdown of the inner BRB on the mean drug concentration in the retina during 6 months for two different values of γ_r, when a intravitreal implant is used.

Intravitreal route

In Figure 11 the behaviour of the drug concentration in the retina during 6 months is represented for $\gamma_r = 10^{-4}$ and $\gamma_r = 10^{-5}$. We observe that a larger γ_r corresponds to a more severe breakdown of the inner BRB. As the concentration peak is a decreasing function of γ_r the result suggests that as diabetic retinopathy progresses the residence time in the retina decreases.

We illustrate now the breakdown of the outer BRB. To understand its influence on the drug concentration in the retina we exhibit in Figure 12 concentration plots for $A_{r,c} = 10^{-8}$ and $A_{r,c} = 10^{-9}$.

We observe that increasing 10 times $A_{r,c}$ does not have a meaningful influence on the behavior of the concentration. Different conclusions will be established for the transscleral route.

Transscleral route

In Figure 13 the behaviour of the drug concentration in the retina during 6 months for $\gamma_r = 10^{-4}, 10^{-5}$ is illustrated. A decreasing of γ_r implies an

The time evolution of the mean concentration in the retina is compared for the two routes in Figure 10, during a six month period. The peak of concentration, 1.48×10^{-3} (mol/mm^3), for the intravitreal implant is achieved after 12 days of release; in the case of the transscleral implant the peak concentration is 1.4×10^{-4} (mol/mm^3) and is attained after 3.8 hours of delivery. We remark that after 6 months the concentration in the case of the intravitreal implant is 3 times higher than the maximum value attained by the transscleral release.

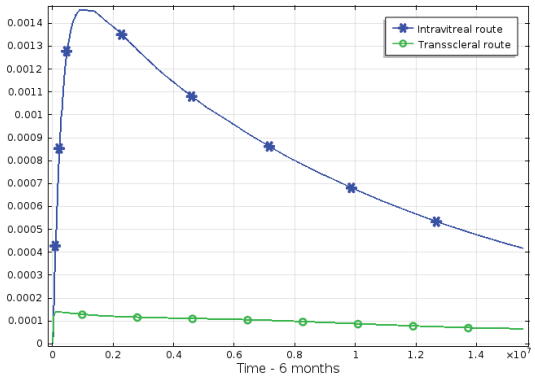

FIGURE 10. Drug concentration in the retina during 6 months: intravitreal route *versus* transscleral route.

It is currently reported in the clinical literature that the intravitreal route leads to higher concentration levels. Our model not only confirms this clinical expectation, but also presents a quantitative comparison of concentrations for both delivery routes.

4.3. Drug release - dependence on pathologies. Blood Retinal Barriers play a central role on the inflow of drug molecules to the posterior ocular tissues and in the outflow of xenobiotics. Alterations of the barrier properties of the BRB's, Figure 3, occur in the most frequent pathologies of the retina. As reported in [1] diabetic retinopathy is initiated by an alteration of the inner BRB and age related macular degeneration is a result of an alteration of the outer BRB. Alterations in the pharmacokinetics of intravitreal drugs in case of age related macular degeneration has been referred in the clinical paper [12].

condition. In each domain the equations include terms that represent the phenomena described in (i)-(v).

We observe that the kinetics in the intravitreal implant is mainly due to the degradation of the polymer and its transport through the device is due to diffusion, with a non constant diffusion coefficient, as described in (i) above. In the vitreo, retina and choroid, pressure gradients may influence drug transport.

(1) Transport in the implant Ω_i

Assuming that only passive transport takes place in the polymeric device, the concentration of drug c_i is described by

$$\frac{\partial c_i}{\partial t} + \nabla.J_i = 0 \text{ in } \Omega_i \times (0,T] \tag{1}$$

where the drug flux J_i is given by $J_i = -D_i\nabla c_i$, and D_i stands for a non linear diffusion coefficient that takes into account the degradation of the polymer. It is defined by $D_i = D_0 exp(k(1 - exp(-k_d c_w t))$ where D_0 represents the diffusion coefficient of the drug in the non hydrolyzed polymer and k stands for the degradation rate ([16]). The constant k_d is a phenomenological constant used to adjust the diffusion coefficient for large times. In the definition of D_i, c_w represents the concentration of water, assumed constant and that is responsible for the polymeric degradation. Assuming that the intravitreal implant swells instantaneously we take $c_w = 1$. In (1) T represents a predefined final time. Drug release from a biodegradable implant has been studied by some of the authors in [10].

(2) Transport in the vitreous Ω_v

The behavior of the drug concentration in the vitreous, c_v, is simulated considering the following equation

$$\frac{\partial c_v}{\partial t} + \nabla.J_v = 0 \text{ in } \Omega_v \times (0,T], \tag{2}$$

where the flux J_v is defined by $J_v = -D_v\nabla c_v + v_v c_v$, D_v stands for the drug diffusion coefficient in the fluid, v_v denotes the convection velocity of aqueous humor given by Darcy's equation

$$\begin{cases} v_v = -\frac{k_v}{\mu_v}\nabla p_v \text{ in } \Omega_v \times (0,T] \\ \nabla.v_v = 0 \text{ in } \Omega_v \times (0,T]. \end{cases} \tag{3}$$

In (3) k_v represents the vitreous permeability and μ_v the viscosity of the fluid. The drug velocity v_v is due to the pressure gradient between the hyaloid membrane Γ_h and the interface $\Gamma_{c,s}$ between the choroid and the sclera. Equation (2) has no sink term because we assumed that the drug is not degraded in the vitreous.

(3) Transport in the retina Ω_r

The retina is considered as a porous medium with permeability k_r where the retinal fluid with viscosity μ_r is transported due to a pressure gradient between the interface $\Gamma_{v,r}$ - that separates the vitreous and the retina - and $\Gamma_{r,c}$ - the interface between the retina and the choroid. Then the convective velocity v_r is defined by

$$\begin{cases} v_r = -\frac{k_r}{\mu_r}\nabla p_r \text{ in } \Omega_r \times (0,T] \\ \nabla . v_r = 0 \text{ in } \Omega_r \times (0,T]. \end{cases} \tag{4}$$

The drug transport in the retina is described by

$$\frac{\partial c_r}{\partial t} + \nabla . J_r = -\gamma_r c_r \text{ in } \Omega_r \times (0,T], \tag{5}$$

where the mass flux in the retina is given by $J_r = -D_r \nabla c_r + (v_r + v_p)c_r$ with v_p standing for a convective term that represents the pumping effect. We observe that once the drug has reached the retina, the outer BRB acts in favor of keeping the level of its concentration in the retina.

The reaction term $-\gamma_r c_r$ in (5) represents the drug clearance that occurs through the inner blood retinal barrier. The term γ_r representes a piecewise function in Ω_r that takes into account the spatial distribution of the retinal capillaries

$$\gamma_r = \begin{cases} \gamma_{r,1} \text{ in } \Omega_{r,1} \\ \gamma_{r,2} \text{ in } \Omega_{r,2}, \end{cases}$$

where $\Omega_r = \Omega_{r,1} \cup \Omega_{r,2}$ with $\Omega_{r,1}$ located approximately at the inner two thirds of the retina. This region is vascularized and served by the retinal blood vessels. The inner BRB consists of retinal capillaries whose endothelial cells are linked by tight junctions. Its function is to feed the first two thirds of the retina while preventing passage of large molecules to the choroid. The function γ_r in the outer one third, $\Omega_{r,2}$, is assumed equal to zero. It is a reasonable approximation because

implant. In this first period of release a higher drug concentration is observed near the implants and, as expected, the highest values are observed for the intravitreal implant. In fact, in the transscleral release, the drug must overcome the inner and the outer BRB and it is also dragged by the blood flow in the choroid, before reaching the vitreous.

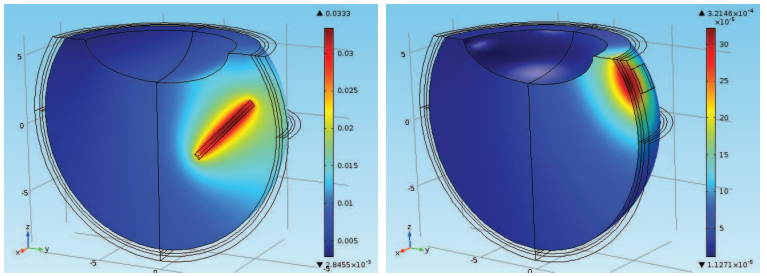

FIGURE 8. Drug concentration in the vitreous after 2 days: intravitreal implant (left) and transscleral implant (right). The scales of the two plots are different.

The concentration of drug does not follow an analogous pattern in the retina (Figure 9): in this case the peak concentration is observed for the transscleral implant, 1.22×10^{-2} (mol/mm^3). However the mean concentration is higher in the retina (7.23×10^{-4} instaed 1.38×10^{-4}) when the intravitreal implant is considered because the minimum values attained are lower in the case of transscleral delivery.

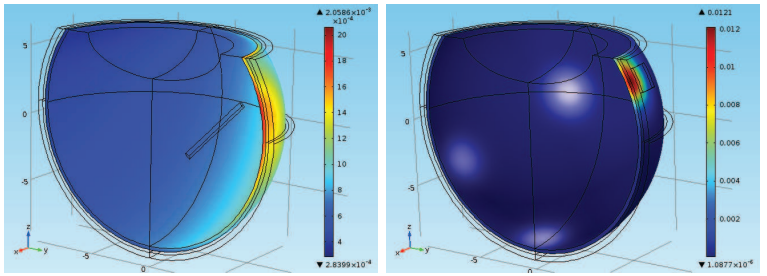

FIGURE 9. Drug concentration in the retina after 2 days: intravitreal implant (left) and transscleral implant (right). The scales of the two plots are different.

are obviously independent of the routes. We observe that the pressure is practically constant in the vitreous chamber, 2000 Pa. It decreases in the retina achieving the mean value of 1822 Pa and abruptly decreases in the choroid to the mean value of 1421 Pa attaining 1200 Pa near the interface choroid/sclera. These results are in agreement with [4], where the pressure in the vitreous was found to be almost uniform, the pressure drop being observed in the retina, choroid, and sclera.

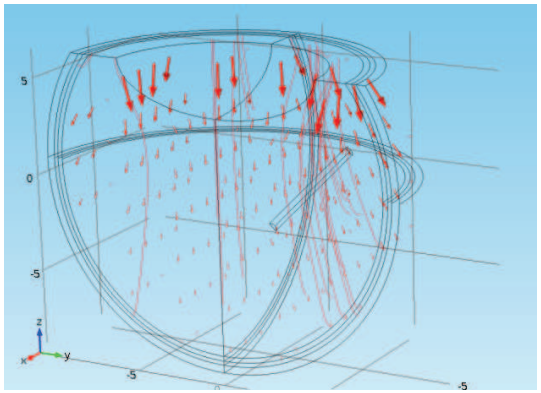

FIGURE 7. Steady state velocity in the vitreous, retina and choroid.

In Figure 7 the convective field is exhibited. As expected the highest values of the fluid velocity are observed near the lens and the hyaloid membrane. The mean velocity in the vitreous is 8.2×10^{-9} (m/s), in the retina it is 3.3×10^{-9} (m/s) and in the choroid it is 3.1×10^{-9} (m/s). These values are in agreement with the literature [4].

4.2. Intravitreal *versus* transscleral routes. In this subsection we illustrate the drug distribution in the vitreous and in the retina when two different routes are used. The implants are made of a biodegradable polymer and they are loaded with the same amount of drug. The behaviour of the mean drug concentration in the retina is compared for the two routes during 6 months.

The drug concentration in the vitreous humor at day 2 is illustrated in Figure 8, left - for the intravitreal implant and right - for the transscleral

there is no vasculature in this domain. An analogous description of the transport in the retina have been used in [5].

(4) Transport in the choroid Ω_c

The choroid provides oxygen and nutrients to the outer part of the retina. It is the vascular tissue of the eye and it is modeled as a highly porous medium where the drug transport is described by

$$\frac{\partial c_c}{\partial t} + \nabla . J_c = -\gamma_c c_c \text{ in } \Omega_c \times (0,T], \tag{6}$$

with $J_c = -D_c \nabla c_c + v_c c_c$ and where v_c is given by

$$\begin{cases} v_c = -\frac{k_c}{\mu_c} \nabla p_c \text{ in } \Omega_c \times (0,T] \\ \nabla . v_c = 0 \text{ in } \Omega_c \times (0,T]. \end{cases} \tag{7}$$

In (7) k_c represents the permeability of the choroid and μ_c the viscosity of the choroidal fluid. In (6) γ_c denotes the clearance rate due to the choroidal blood flow.

(5) Transport in the sclera Ω_c

The sclera is the outer layer of the eye containing collagen and elastic fibers. Assuming that only passive transport takes place in the sclera, the concentration of drug c_s is described by

$$\frac{\partial c_s}{\partial t} + \nabla . J_s = 0 \text{ in } \Omega_s \times (0,T], \tag{8}$$

where $J_s = -D_s \nabla c_s$ and D_s stands for the diffusion coefficient of the drug in the sclera.

To close the system (1)-(8) we add interface, boundary (Figure 5) and initial conditions.

For the concentration the following conditions are used

(1) On the boundary $\Gamma_v = \Gamma_\ell \cup \Gamma_h$, that borders the lens and the hyaloid membrane, two different conditions are considered.

As no drug flux permeates Γ_ℓ we consider the null flux condition

$$J_v . \eta_v = 0 \text{ on } \Gamma_\ell \times (0,T], \tag{9}$$

where η_v is the exterior unitary normal to Ω_v on Γ_ℓ.

Regarding the boundary Γ_h, between that separates the hyaloid from the anterior chamber, it is known that there is a rapid turnover of aqueous humor in the anterior chamber and that all molecules in the

vitreous humor can move across the hyaloid membrane ([17]). To mimic this forward clearance we consider

$$J_v.\eta_v = A_h c_v \text{ on } \Gamma_h \times (0,T], \tag{10}$$

where A_h denotes the drug transfer coefficient at this boundary.

(2) We assume that no drug flux crosses the top of the retina Γ_r, choroid Γ_c and sclera $\Gamma_{s'}$:

$$J_r.\eta_r = 0 \text{ on } \Gamma_r \times (0,T], J_c.\eta_c = 0 \text{ on } \Gamma_c \times (0,T], J_s.\eta_s = 0 \text{ on } \Gamma_{s'} \times (0,T], \tag{11}$$

where η_r, η_c and η_s are the exterior unitary normal to Ω_r on Γ_r, Ω_c on Γ_c, Ω_s on $\Gamma_{s'}$, respectively.

(3) On the interface $\Gamma_{i,v}$ between the implant and the vitreous:
We assume the continuity of the flux and its dependence on the permeability of $\Gamma_{i,v}$ that is

$$J_i.\eta_i = -J_v.\eta_v,\ J_i.\eta_i = A_{i,v}(c_i - c_v) \text{ on } \Gamma_{i,v} \times (0,T]. \tag{12}$$

In (12) η_i represents the exterior unitary normal to Ω_i on $\Gamma_{i,v}$ and $A_{i,v}$ stands for the partition coefficient.

(4) On the interface $\Gamma_{v,r}$ between the vitreous and the retina:
We assume the following conditions

$$J_v.\eta_v = -J_r.\eta_r,\ J_v.\eta_v = A_{v,r}(c_v - c_r) \text{ on } \Gamma_{v,r} \times (0,T], \tag{13}$$

where η_r represents the exterior unitary normal to Ω_r on $\Gamma_{v,r}$ and $A_{v,r}$ stands for the permeability coefficient.

(5) On the interface $\Gamma_{r,c}$ between the retina and the choroid:
We assume as before

$$J_r.\eta_r = -J_c.\eta_c,\ J_r.\eta_r = A_{r,c}(c_r - c_c) \text{ on } \Gamma_{r,c} \times (0,T], \tag{14}$$

where η_c represents the exterior unitary normal to Ω_c on $\Gamma_{r,c}$ and $A_{r,c}$ stands for the permeability coefficient.

(6) On the interface $\Gamma_{c,s}$ between the choroid and the sclera:
The following conditions are assumed

$$J_c.\eta_c = -J_s.\eta_s,\ J_c.\eta_c = A_{c,s}(c_c - c_s) \text{ on } \Gamma_{c,s} \times (0,T], \tag{15}$$

where η_s represents the exterior unitary normal to Ω_s on $\Gamma_{c,s}$ and $A_{c,s}$ stands for the permeability coefficient.

The numerical simulations are obtained with $c_0 = 1.7887 \times 10^{-6}$ (mol/mm^3), which represents the initial drug concentration in the implants and $k_d = 1$ $(1/s)$. All the tissues are considered isotropic. The diffusion of the drug in the non hydrolyzed polymer is defined in (m^2/s) by $D_i = D_0 exp(k(1 - exp(-k_d c_w t))$ with $D_0 = 10^{-13}$; its diffusion coefficient in the permeating fluid (aqueous humor and liquefied vitreous humor) is defined by $D_v = 5 \times 10^{-10}$, $D_r = 3.9 \times 10^{-11}$, $D_c = D_s = 10^{-10}$ respectively in the vitreous, retina and sclera. These drug diffusion coefficients correspond to dexamethasone ([4]). We recall that the diffusion coefficient in the polymer will increase as the molecular weight decreases, that is as degradation occurs. The values of the parameters have been gathered from [3], [4], [13] and are presented in Table I.

Table I: Value of the model parameters used in the numerical simulations.

Parameter	Value	Unit	Description
c_0	1.7887×10^{-6}	mol/mm^3	initial drug concentration in the implant
D_i	10^{-10}	m^2/s	drug diffusion coef. in the implant
D_v	5×10^{-10}	m^2/s	drug diffusion coef. in the vitreous
D_r	3.9×10^{-11}	m^2/s	drug diffusion coef. in the retina
D_c	10^{-10}	m^2/s	drug diffusion coef. in the choroid
D_s	10^{-10}	m^2/s	drug diffusion coef. in the sclera
(k_v/μ_r)	8.4×10^{-11}	$m^2/Pa.s$	hydraulic conductivity in the vitreous
(k_r/μ_c)	2.36×10^{-15}	$m^2/Pa.s$	hydraulic conductivity in the retina
(k_c/μ)	1.5×10^{-15}	$m^2/Pa.s$	hydraulic conductivity in the choroid
$A_{i,v}$	10^{-11}	m/s	Permeability coefficient at $\Gamma_{i,v}$
$A_{v,r}$	10^{-8}	m/s	Permeability coefficient at $\Gamma_{v,r}$
$A_{r,c}$	10^{-8}	m/s	Permeability coefficient at $\Gamma_{r,c}$
$A_{c,s}$	10^{-7}	m/s	Permeability coefficient at $\Gamma_{c,s}$
A_h	6×10^{-8}	m/s	Permeability coefficient at Γ_h
A_c	6×10^{-8}	m/s	Permeability coefficient at Γ_s
$\gamma_{r,1}$	10^{-4}	$1/s$	drug clearance coefficient in the retina
γ_c	10^{-4}	$1/s$	drug clearance coefficient in the choroid
v_p	3.1×10^{-8}	m/s	convective pumping effect in the retina

4.1. Pressure and velocity in the vitreous chamber. The transport in the vitreous is due to diffusion and convection. The vitreous is a porous media and the pressure gradient - induced by the difference between the intra-ocular pressure in the anterior chamber and the pressure in the choroid - creates a convective field. We use Darcy's law to define the convective field of the aqueous humor flow and the pressure distribution. The results are the same for both routes of administration because pressure and convection

Following [18] the existence of solution of the weak problem (26) is a direct consequence of the stablity estimate (35) and of the generalized coercivity condition (36).

4. Numerical Simulations

In this section we analyze the behavior of drug concentration in the retina using the two types of administration previously described: an intravitreal implant (subsection 2.2.1) and a transscleral implant (subsection 2.2.2). To follow the path of drug flow, we present plots of concentration in the implant, the vitreous humor and the retina in the case of the intravitreal implant; in the implant, sclera, choroid and retina in the case of the transscleral implant. The residence time and the concentration peak are evaluated. The influence of the leakage of BRB's is also illustrated.

The models presented are tridimensional and the domain represents half of the vitreous chamber of the eye. We assume that this domain contains half of the implant. The numerical results are obtained with *COMSOL Multiphysics*, using a piecewise finite element method, linear for the velocity and the pressure and quadratic for the concentrations. A triangulation automatically generated with 205239 elements is used. In the case of an intravitreal implant, the triangulation is represented in Figure 6. To integrate in time, adaptive Backward Differentiation Formulae, with orders between 1 and 2 and adaptive time step are used.

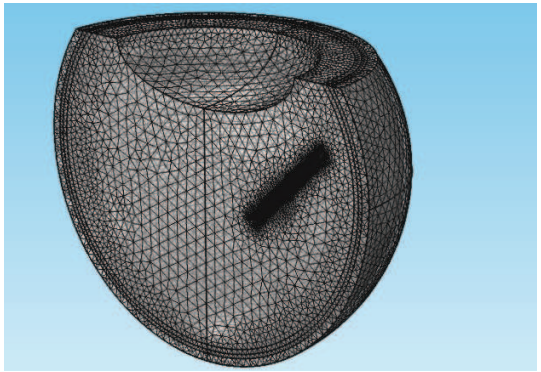

FIGURE 6. Mesh for the intravitreal implant with 205239 elements.

(7) On the exterior boundary Γ_s of the sclera:
To describe the loss of drug that occurs from the scleral surface through the episcleral veins, we consider that at Γ_s we have

$$J_s.\eta_s = A_s c_s \text{ on } \Gamma_s \times (0,T], \tag{16}$$

where η_s represents the exterior unitary normal to Ω_s on Γ_s and A_s denotes the drug transfer coefficient on the scleral surface.

To compute the convective velocity induced by the pressure gradient we consider the following boundary conditions:

(1) On the hyaloid membrane Γ_h:

$$p = 2000Pa \text{ on } \Gamma_h \times (0,T]. \tag{17}$$

This value corresponds to a normal intraocular pressure.

(2) On the boundary $\Gamma_{i,v}$ of the implant:

$$v_v.\eta_v = 0 \text{ on } \Gamma_{i,v} \times (0,T]. \tag{18}$$

(3) On the interface $\Gamma_{v,r}$ between the vitreous and the retina:

$$p_v = p_r,\ v_v.\eta_v = -v_r.\eta_r \text{ on } \Gamma_{v,r} \times (0,T]. \tag{19}$$

(4) On the interface $\Gamma_{r,c}$ between the retina and the choroid:

$$p_r = p_c,\ v_r.\eta_r = -v_c.\eta_c \text{ on } \Gamma_{r,c} \times (0,T]. \tag{20}$$

(5) Following [2] we will assume that for a normal adult the pressure on $\Gamma_{c,s}$ is 1200 Pa, that is on the interface $\Gamma_{c,s}$ between the choroid and the sclera,

$$p_c = 1200Pa \text{ on } \Gamma_{c,s} \times (0,T]. \tag{21}$$

Finally, initial conditions need to be imposed. We assume that

$$c_i(0) = c_0 \text{ in } \Omega_i,\ c_j(0) = 0 \text{ in } \Omega_j,\ j = v,r,c,s. \tag{22}$$

2.2.2. *Drug release from a transscleral implant.* We consider now a transscleral implant where the drug has been dispersed (Figure 4-rigth). There is no single pathway after the drug has passed across the sclera. The drug may permeate the retina via the anterior chamber, the systemic circulation or the direct penetration pathway. Previous laboratorial studies have revealed that the dominant pathway is direct penetration, while recirculation or movement from the aqueous to vitreous chambers are not significant ([6]). In this paper we focus on the direct pathway.

In the case of drug delivery from a transscleral implant the main phenomena occurring before the drug reaches the retina are summarized in what follows:

(i) In the transscleral implant (Ω_i): drug diffusion, biodegradation of the polymer;
(ii) In the sclera (Ω_s): drug diffusion and clearance;
(iii) In the choroid (Ω_c): diffusion and clearance due to the high choroidal blood flow that drags a large amount of drug before it reaches the retina;
(iv) In the interface choroid/retina: hindered permeation through the outer BRB that is the Retinal Pigment Epithelium and opposition of the efflux pumping.
(v) In the vitreous (Ω_v) and in the retina (Ω_r): diffusion and convection.

The equations that describe the path of the drug are the same as those presented in the previous subsection. We note that contrarily to what happens with the transport of drug, released intravitreally, in the case of transscleral delivery the outer BRB and the efflux pumping represent barriers that oppose the entrance of drug in the retina.

The boundary condition (16) in this case holds only at Γ_s $\Gamma_{i,s}$, where $\Gamma_{i,s}$ represents the interface between the sclera and the transscleral implant, and on $\Gamma_{i,s}$ we assume

$$J_i.\eta_i = -J_s.\eta_s,\ J_i.\eta_i = A_{i,s}(c_i - c_s) \text{ on } \Gamma_{i,s}\times(0,T], \tag{23}$$

where $A_{i,s}$ denotes the drug transfer coefficient at the interface $\Gamma_{i,s}$, and J_i represents in this case the drug flux in the transscleral implant. In (23) η_i represents the exterior unitary normal to Ω_i on $\Gamma_{i,s}$.

3. Weak solution of the coupled IBVP

In this section we introduce the weak formulation of the drug release problem from the intravitreal implant defined in section 2.2.1 and we prove the existence of solution. A similar result can be obtained for the transscleral implant problem.

We represent by $L^2(\Omega_j)$, $H^1(\Omega_j)$, $j = i, v, r, c, s$, and $L^2(\Gamma)$, $\Gamma \in \{\Gamma_h, \Gamma_r, \Gamma_c, \Gamma_{s'}, \Gamma_{i,v}, \Gamma_{v,r}, \Gamma_{r,c}, \Gamma_{c,s}, \Gamma_s\}$, the usual Sobolev spaces. The usual L^2- inner product is denoted by $(.,.)_{L^2}$ and the corresponding norm is denoted by $\|.\|_{L^2}$.

Weak formulation for the concentration

Then from (32) we conclude that the function

$$\begin{aligned} &e^{2\gamma t}\|c(t)\|_L^2 + \int_0^t e^{2\gamma s}\hat{D}_j\|\nabla c_j(s)\|^2_{[L^2(\Omega_j)]^3}ds \\ &\quad + \min\{A_{i,v}, A_{v,r}, A_{r,c}, A_{c,s}, A_h, A_s\} \\ &\int_0^t e^{2\gamma\omega}\Big(\|c_i(\omega) - c_v(\omega)\|^2_{L^2(\Gamma_{i,v})} + \|c_v(\omega) - c_r(\omega)\|^2_{L^2(\Gamma_{v,r})} \\ &+\|c_r(\omega) - c_c(\omega)\|^2_{L^2(\Gamma_{r,c})} + \|c_c(\omega) - c_s(\omega)\|^2_{L^2(\Gamma_{c,s})} \\ &+\|c_v(\omega)\|^2_{L^2(\Gamma_h)} + \|c_s(\omega)\|^2_{L^2(\Gamma_s)}\Big)d\omega \end{aligned} \tag{34}$$

is decreasing in $[0,T]$, where

$$\begin{aligned} \gamma = \min\{&-\frac{1}{4\epsilon_v^2}\|v_v\|^2_{L^\infty(\Omega_v)}, -\frac{1}{4\epsilon_c^2}\|v_c\|^2_{L^\infty(\Omega_c)} + \|\gamma_c\|_{L^\infty(\Omega_c)}, \\ &-\frac{1}{4\epsilon_r^2}\Big(\|v_p\|^2_{L^\infty(\Omega_r)} + \|v_r\|^2_{L^\infty(\Omega_j)}\Big) + \|\gamma_r\|_{L^\infty(\Omega_r)}\}. \end{aligned}$$

From (34) we obtain

$$\begin{aligned} &\|c(t)\|_L^2 + \int_0^t e^{2\gamma(\omega-t)}\hat{D}_j\|\nabla c_j(\omega)\|^2_{[L^2(\Omega_j)]^3}d\omega \\ &\quad + \min\{A_{i,v}, A_{v,r}, A_{r,c}, A_{c,s}, A_h, A_s\} \\ &\int_0^t e^{2\gamma(\omega-t)}\Big(\|c_i(\omega) - c_v(\omega)\|^2_{L^2(\Gamma_{i,v})} + \|c_v(\omega) - c_r(\omega)\|^2_{L^2(\Gamma_{v,r})} \\ &+\|c_r(\omega) - c_c(\omega)\|^2_{L^2(\Gamma_{r,c})} + \|c_c(\omega) - c_s(\omega)\|^2_{L^2(\Gamma_{c,s})} \\ &+\|c_v(\omega)\|^2_{L^2(\Gamma_h)} + \|c_s(\omega)\|^2_{L^2(\Gamma_s)}\Big)d\omega \\ &\quad \le e^{-2\gamma t}\|c_i(0)\|^2_{L^2(\Omega_i)}, \quad t\in[0,T]. \end{aligned} \tag{35}$$

As $-\gamma > 0$ we conclude from estimate (35) that the function (34) is decreasing and bounded in $(0,T)$.

It is easy to show that there exists a positive constant α_0 and $\sigma \in \mathbb{R}$ such that

$$\begin{aligned} a_c(u,u) + \sigma &\sum_{j=i,v,r,c,s}\|u_j\|^2_{L^2(\Omega_j)} \\ &\ge \alpha_0\sum_{j=i,v,r,c,s}\|u_j\|^2_{H^1(\Omega_j)},\ \forall u \in \prod_{j=i,v,r,c,s}H^1(\Omega_j). \end{aligned} \tag{36}$$

In this case we easily conclude that

$$\begin{aligned}\|c(t)\|_L^2 \; &+ \sum_{j=i,v,r,c,s} D_j \int_0^t e^{2\gamma(\omega-t)} \|\nabla c_j(\omega)\|^2_{[L^2(\Omega_j)]^3} d\omega \\ &+ \min\{A_{i,v}, A_{v,r}, A_{r,c}, A_{c,s}, A_h, A_s\} \\ &\int_0^t e^{2\gamma(\omega-t)} \Big(\|c_i(\omega) - c_v(\omega)\|^2_{L^2(\Gamma_{i,v})} + \|c_v(\omega) - c_r(\omega)\|^2_{L^2(\Gamma_{v,r})} \\ &\quad + \|c_r(\omega) - c_c(\omega)\|^2_{L^2(\Gamma_{r,c})} + \|c_c(\omega) - c_s(\omega)\|^2_{L^2(\Gamma_{c,s})} \\ &\quad + \|c_v(\omega)\|^2_{L^2(\Gamma_h)} + \|c_s(\omega)\|^2_{L^2(\Gamma_s)} \Big) d\omega \\ &\quad \leq e^{-2\gamma t} \|c_i(0)\|^2_{L^2(\Omega_i)}, \quad t \in [0,T],\end{aligned}$$

where $\gamma = \min_{j=r,c} \|\gamma_j\|_{L^\infty(\Omega_j)}$. However, in the presence of convective transport we observe that for $\epsilon_j \neq 0$, $j = v, r, c$, from (31), we get

$$\begin{aligned}\tfrac{1}{2}\tfrac{d}{dt}\|c(t)\|_L^2 \; &+ \sum_{j=i,s} D_j \|\nabla c_j(t)\|^2_{[L^2(\Omega_j)]^3} + \sum_{j=v,c} \Big(D_j - \epsilon_j^2 \Big) \|\nabla c_j(t)\|^2_{[L^2(\Omega_j)]^3} \\ &+ \Big(D_r - 2\epsilon_r^2 \Big) \|\nabla c_r(t)\|^2_{[L^2(\Omega_r)]^3} - \sum_{j=v,c} \frac{1}{4\epsilon_j^2} \|v_j\|^2_{L^\infty(\Omega_j)} \|c_j(t)\|^2_{L^2(\Omega_j)} \\ &- \frac{1}{4\epsilon_r^2} \Big(\|v_p\|^2_{L^\infty(\Omega_r)} + \|v_r\|^2_{L^\infty(\Omega_j)} \Big) \|c_r(t)\|^2_{L^2(\Omega_r)} \\ &\leq - \min\{A_{i,v}, A_{v,r}, A_{r,c}, A_{c,s}, A_h, A_s\} \\ &\quad \Big(\|c_i(t) - c_v(t)\|^2_{L^2(\Gamma_{i,v})} + \|c_v(t) - c_r(t)\|^2_{L^2(\Gamma_{v,r})} \\ &\quad + \|c_r(t) - c_c(t)\|^2_{L^2(\Gamma_{r,c})} + \|c_c(t) - c_s(t)\|^2_{L^2(\Gamma_{c,s})} \\ &\quad + \|c_v(\omega)\|^2_{L^2(\Gamma_h)} + \|c_s(\omega)\|^2_{L^2(\Gamma_s)} \Big) - \sum_{j=r,c} \|\gamma_j\|_{L^\infty(\Omega_j)} \|c_j\|^2_{L^2(\Omega_j)}.\end{aligned} \tag{32}$$

Let ϵ_j be fixed by

$$\hat{D}_j = 2(D_j - \epsilon_j^2) > 0, j = v, c, \;\; \hat{D}_r = 2(D_r - 2\epsilon_r^2) > 0. \tag{33}$$

To define the weak formulation we start by considering the weak problem for the concentration $c_i(t)$ in the implant (Ω_i). We assume that the concentration $c_i(t)$ is known on $\Gamma_{i,v}$. The weak formulation of the differential problem (2) complemented by the boundary condition defined by the second condition of (12) is defined by: find $c_i(t) \in H^1(\Omega_i)$ such that $\dfrac{\partial c_i}{\partial t}(t) \in L^2(\Omega_i)$, $c_i(0) = c_0$ and

$$\begin{aligned}&(\frac{\partial c_i}{\partial t}(t), w_i)_{L^2(\Omega_i)} + (D_i(t)\nabla c_i(t), \nabla w_i)_{[L^2(\Omega_i)]^3} \\ &= -A_{i,v}(c_i(t) - c_v(t), w_i)_{L^2(\Gamma_{i,v})}, \; \forall w_i \in H^1(\Omega_i).\end{aligned} \tag{24}$$

If we assume that $c_i(t)$ and $c_r(t)$ are known functions in $\Gamma_{i,v}$ and $\Gamma_{v,r}$ respectively, for the vitreous body we define an analogous weak formulation: find $c_v(t) \in H^1(\Omega_v)$ such that $\dfrac{\partial c_v}{\partial t}(t) \in L^2(\Omega_v)$, $c_v(0) = 0$ and

$$\begin{aligned}&(\frac{\partial c_v}{\partial t}(t), w_v)_{L^2(\Omega_v)} - (v_v c_v, \nabla w_v)_{[L^2(\Omega_v)]^3} + (D_v \nabla c_v(t), \nabla w_v)_{[L^2(\Omega_v)]^3} \\ &= -A_h(c_v(t), w_v)_{L^2(\Gamma_h)} + A_{i,v}(c_i(t) - c_v(t), w_v)_{L^2(\Gamma_{i,v})} \\ &- A_{v,r}(c_v(t) - c_r(t), w_v)_{L^2(\Gamma_{v,r})}, \; \forall w_v \in H^1(\Omega_v).\end{aligned} \tag{25}$$

Defining analogously the weak problems for the concentration in the retina, choroid and sclera we introduce the complete weak problem for the coupled concentration problem: find $c(t) = (c_i(t), c_v(t), c_r(t), c_c(t), c_s(t))$, $c(t) \in H_c = \prod_{j=i,v,r,c,s} H^1(\Omega_j)$ such that $\dfrac{\partial c}{\partial t}(t) \in L = \prod_{j=i,v,r,c,s} L^2(\Omega_j)$ with $c(0) = (c_0, 0, 0, 0, 0)$ and

$$(\frac{\partial c}{\partial t}(t), w)_L + a_c(c(t), w) = 0, \; \forall w \in H_c. \tag{26}$$

In (26)

$$(w, u)_L = \sum_{j=i,v,r,c,s} (w_j, u_j)_{L^2(\Omega_j)},$$

for $w, u \in L = \prod_{j=i,v,r,c,s} L^2(\Omega_j)$ and $a_c(.,.) : H \times H \to \mathbb{R}$ with

$$\begin{aligned} a(w,u) &= \sum_{j=i,v,r,c,s} (D_j\nabla w_j, \nabla u_j)_{[L^2(\Omega_j)]^3} \\ &- \sum_{j=v,r,c} (v_j w_j, \nabla u_j)_{[L^2(\Omega_j)]^3} - (v_p w_r, \nabla u_r)_{[L^2(\Omega_r)]^3} \\ &+A_{i,v}(w_i(t)-w_v(t), u_i-u_v)_{L^2(\Gamma_{i,v})} + A_{v,r}(w_v(t)-w_r(t), u_v-u_r)_{L^2(\Gamma_{v,r})} \\ &+A_{r,c}(w_r(t)-w_c(t), u_r-u_c)_{L^2(\Gamma_{r,c})} + A_{c,s}(w_c(t)-w_s(t), u_c-u_s)_{L^2(\Gamma_{c,s})} \\ &+A_h(w_v(t),u_v)_{L^2(\Gamma_h)} + A_s(w_s(t),u_s)_{L^2(\Gamma_s)} + \sum_{j=r,c}(\gamma_j w_j, u_j)_{L^2(\Omega_j)}, \end{aligned} \tag{27}$$

for $w, u \in H$.

Weak formulation for the pressure

To define the weak problem for the pressure, we introduce the space $\prod_{j=v,r,c} H^1(\Omega_j)$ and we define

$$H_p = \{z \in \prod_{j=v,r,c} H^1(\Omega_j) : z_v = 0 \text{ on } \Gamma_h,\ z_c = 0 \text{ on } \Gamma_{c,s}\}.$$

The following weak problem is considered: find $p = (p_v, p_r, p_c)$, $p \in \prod_{j=v,r,c} H^1(\Omega_j)$ such that $p_v = p0v$ on Γ_h, $p_c = p0cPa$ on $\Gamma_{c,s}$ and

$$a_p(p,q) = 0, \forall q \in H_p, \tag{28}$$

where $a_p(.,.) : H_p \times H_p \to \mathbb{R}$, with

$$a_p(z,q) = \sum_{j=v,r,c} (\frac{k_j}{\mu_j}\nabla z, \nabla q)_{L^2(\Omega_j)}$$

for $z, q \in H_p$.

The variational pressure problem (28) is solved introducing a function $\hat{p} \in \prod_{j=v,r,c} H^1(\Omega_j)$ such that $\hat{p}_v = \hat{p}_v 0$ on Γ_h, $\hat{p}_c = \hat{p}_c 0$ on $\Gamma_{c,s}$ and find $\tilde{p} \in H_p$ such that

$$a_p(\tilde{p}, z) = -a_p(\hat{p}, z), \quad \forall z \in H_p. \tag{29}$$

Then we take $p = \tilde{p} + \hat{p}$.

3.1. Well-pondness of concentration. We establish in what follows energy estimates for the solutions of the weak problems (26) and (29).

Let us begin with problem (29). As $a_p(.,.)$ is an elliptic bilinear form in $[H_p]^2$ we conclude that, for each $\hat{p} \in H_p$, there exists a unique $\tilde{p} \in H_p$ satisfying (29). It can be shown, using standard techniques, that such solution is bounded as follows

$$\sum_{j=v,r,c} \|\nabla p_j\|^2_{[L^2(\Omega_j)]^3} \leq \Big(\frac{\frac{1}{2\epsilon^2}\max_{j=v,r,c}\frac{K_j^2}{\mu_j^2}}{\min_{j=v,r,c}\frac{K_j}{\mu_j} - \epsilon^2} + 2\Big) \sum_{j=v,r,c} \|\nabla \hat{p}_j\|^2_{[L^2(\Omega_j)]^3} \tag{30}$$

where ϵ is such that $\min_{j=v,r,c}\frac{K_j}{\mu_j} - \epsilon^2 > 0$.

Regarding weak formulation (26) , by taking $w = c(t)$ we get

$$\begin{aligned} \tfrac{1}{2}\tfrac{d}{dt}\|c(t)\|^2_L &+ \sum_{j=i,v,r,c,s} D_j\|\nabla c_j(t)\|_{[L^2(\Omega_j)]^3} \\ &- \sum_{j=v,r,c} (v_j c_j(t), \nabla c_j(t))_{[L^2(\Omega_j)]^3} - (v_p c_r(t), \nabla c_r(t))_{[L^2(\Omega_r)]^3} \\ &\leq -\min\{A_{i,v}, A_{v,r}, A_{r,c}, A_{c,s}, A_h, A_s\} \\ &\quad \Big(\|c_i(t)-c_v(t)\|^2_{L^2(\Gamma_{i,v})} + \|c_v(t)-c_r(t)\|^2_{L^2(\Gamma_{v,r})} \\ &\quad +\|c_r(t)-c_c(t)\|^2_{L^2(\Gamma_{r,c})} + \|c_c(t)-c_s(t)\|^2_{L^2(\Gamma_{c,s})} \\ &\quad +\|c_v(t)\|^2_{L^2(\Gamma_h)} + \|c_s(t)\|^2_{L^2(\Gamma_s)}\Big) - \sum_{j=r,c}\|\gamma_j\|_{L^\infty(\Omega_j)}\|c_j(t)\|^2_{L^2(\Omega_j)}, \end{aligned} \tag{31}$$

where $\|.\|_{L^\infty(\Omega_j)}$ represents the usual norm in $L^\infty(\Omega_j)$, $j = r, c$.

In absence of convective flux we observe that

$$\|c(t)\|^2_L + 2\sum_{j=i,v,r,c,s} D_j \int_0^t \|\nabla c_j(\omega)\|^2_{[L^2(\Omega_j)]^3} d\omega$$

is a decreasing function with a decreasing rate given by $-2\min\{A_{i,v}, A_{v,r}, A_{r,c}, A_h, A_s, \gamma_r, \gamma_c\}$.